Next-To-Leading Order QCD Corrections to $pp \to t\bar{t}b\bar{b} + X$ at the LHC

A. Bredenstein,[1] A. Denner,[2] S. Dittmaier,[3,4] and S. Pozzorini[5]

[1]*High Energy Accelerator Research Organization (KEK), Tsukuba, Ibaraki 305-0801, Japan*
[2]*Paul Scherrer Institut, Würenlingen und Villigen, CH-5232 Villigen PSI, Switzerland*
[3]*Albert-Ludwigs-Universität Freiburg, Physikalisches Institut, D-79104 Freiburg, Germany*
[4]*Max-Planck-Institut für Physik (Werner-Heisenberg-Institut), D-80805 München, Germany*
[5]*CERN, CH-1211 Geneva 23, Switzerland*

(Received 1 May 2009; published 1 July 2009)

We report on the calculation of the full next-to-leading-order QCD corrections to the production of $t\bar{t}b\bar{b}$ final states at the LHC, which deliver a serious background contribution to the production of a Higgs boson (decaying into a $b\bar{b}$ pair) in association with a $t\bar{t}$ pair. While the corrections significantly reduce the unphysical scale dependence of the leading-order cross section, our results predict an enhancement of the $t\bar{t}b\bar{b}$ production cross section by a K factor of about 1.8.

DOI: 10.1103/PhysRevLett.103.012002 PACS numbers: 14.65.Ha

Extending earlier work [1], where we discussed the next-to-leading-order (NLO) QCD corrections to $t\bar{t}b\bar{b}$ production via quark-antiquark annihilation, in this Letter we present first results on the full NLO QCD corrections to $pp \to t\bar{t}b\bar{b} + X$ at the LHC; i.e., we complete the existing results by the contributions from gluonic initial states.

The QCD-initiated production of $t\bar{t}b\bar{b}$ final states represents a very important background to $t\bar{t}H$ production where the Higgs boson decays into a $b\bar{b}$ pair. While early studies of $t\bar{t}H$ production at ATLAS [2] and CMS [3] suggested even discovery potential of this process for a light Higgs boson, more recent analyses [4–7] with more realistic background assessments show that the signal significance is jeopardized if the background from $t\bar{t}b\bar{b}$ and $t\bar{t}$ + jets final states is not controlled very well. The calculation presented in this Letter renders improved signal and background studies possible that are based on NLO predictions for $t\bar{t}b\bar{b}$ final states. NLO QCD corrections are already available for the $t\bar{t}H$ signal [8–11] and the background from $t\bar{t}$ + jet [12,13] and $t\bar{t}Z$ [14].

On the theoretical side, the calculation of NLO corrections to $2 \to 4$ particle processes represents the current technical frontier. The complexity of such calculations triggered the creation of prioritized experimenters' wishlists [15,16] for missing NLO calculations for LHC physics, and the process of $t\bar{t}b\bar{b}$ production ranges among the most wanted candidates. In recent years the field of NLO calculations to multiparticle processes received an enormous boost, most notably by advanced methods for evaluating one-loop tensor integrals for Feynman diagrams [17–23] and by new methods employing unitarity cuts of one-loop amplitudes analytically (see, e.g., Ref. [24] and references therein) or numerically [25–30]. The numerical unitarity-based approaches have successfully passed their proof of principle in the calculation of specific one-loop QCD amplitudes, including, in particular, multigluon amplitudes [30–32], $u\bar{d} \to W^+ q\bar{q}g$ [33], $u\bar{d} \to W^+ ggg$ [33,34], $u\bar{u}/gg \to t\bar{t}b\bar{b}$, $u\bar{u} \to W^+W^-b\bar{b}$, $u\bar{u} \to b\bar{b}b\bar{b}$, $u\bar{u}/gg \to t\bar{t}gg$ [34], and in the evaluation of the leading-color contribution at NLO to W + 3jet production at the Tevatron [33,35,36]. The Feynman-diagrammatic approach has already been used in complete NLO predictions for some $2 \to 4$ reactions at e^+e^- [37,38] and $\gamma\gamma$ colliders [39] and in the evaluation of the amplitude of $q\bar{q} \to b\bar{b}b\bar{b}$ [40] at one loop. The evaluation of $t\bar{t}b\bar{b}$ production—also based on Feynman diagrams, as documented in Ref. [1] and this Letter—represents the first full NLO calculation for a $2 \to 4$ process at a hadron collider.

In LO QCD, 7 and 36 different Feynman diagrams contribute to the production of $t\bar{t}b\bar{b}$ final states via $q\bar{q}$ annihilation and gg fusion, respectively. The virtual QCD corrections comprise about 200 one-loop diagrams for the $q\bar{q}$ and about 1000 diagrams for the gg initial state, the most complicated being the 8 and 40 hexagons for the respective channels. Some hexagon graphs are depicted in Fig. 1. The real QCD corrections comprise gluon bremsstrahlung in the $q\bar{q}$ and gg channels, $q\bar{q}/gg \to t\bar{t}b\bar{b}g$, and

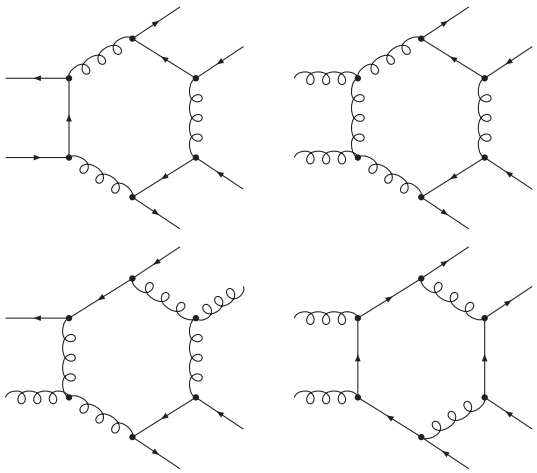

FIG. 1. Some generic hexagon diagrams for hadronic $t\bar{t}b\bar{b}$ production at NLO QCD.

(anti)quark–gluon scattering processes, $\overset{(-)}{q}\, g \to t\bar{t}b\bar{b}\,\overset{(-)}{q}$. We consistently neglect contributions involving b quarks in the initial state because of their suppression in the parton distribution functions (PDFs). In the following we briefly describe the calculation of the virtual and real corrections. Each of these contributions has been worked out twice and independently, resulting in two completely independent computer codes.

The evaluation of the virtual corrections starts with the generation of the one-loop amplitudes via two independent versions of FEYNARTS [41,42]. Using either inhouse MATHEMATICA routines or FORMCALC [43], each diagram is decomposed in terms of standard spin and color structures, as described in Ref. [1] for the $q\bar{q}$ channel in detail. The coefficients in the resulting linear combination of these standard structures contain the one-loop tensor integrals. The obtained expressions are not reduced to standard scalar integrals analytically, but the tensor integrals are evaluated by means of algorithms that perform a recursive reduction to master integrals in numerical form. This avoids a further increase of the huge analytic expressions and permits to adapt the reduction strategy to the specific numerical problems that appear in different phase-space regions. In detail, the 6-/5-point integrals are directly expressed in terms of 5-/4-point integrals [18,22]. Tensor 4-point and 3-point integrals are reduced to standard scalar integrals with the Passarino–Veltman algorithm [44] as long as no small Gram determinant appears in the reduction. If small Gram determinants occur, the alternative schemes of Ref. [22] are applied. Ultraviolet (UV) divergences are regularized dimensionally throughout, but infrared (IR) divergences are treated in different variants, which comprise pure dimensional regularization with strictly massless light quarks (including b quarks) and a hybrid scheme with small quark masses. The corresponding scalar master integrals are evaluated using the methods and results of Refs. [45,46], where different regularization schemes are translated into each other as described in Ref. [47]. Our treatment of rational terms of UV or IR origin is described in appendix A of Ref. [1]. More details on the two independent calculations of the virtual corrections in the gg channel will be presented elsewhere.

In both evaluations of the real corrections the amplitudes are calculated in the form of helicity matrix elements which have been generated with MADGRAPH 4.1.33 [48]. While the amplitudes for $q\bar{q} \to t\bar{t}b\bar{b}g$ have been checked with the spinor formalism of Ref. [49], those for $gg \to t\bar{t}b\bar{b}g$ have been verified with an implementation of off-shell recursion relations [50–52]. The singularities for soft or collinear gluon emission are isolated via dipole subtraction [53–56] for NLO QCD calculations using the formulation [53] for massive quarks. One of the two calculations employs the automatic MADDIPOLE implementation of dipole subtraction [57]. After combining virtual and real corrections, singularities connected to collinear configurations in the final state cancel for "collinear-safe" observables after applying a jet algorithm. Singularities connected to collinear initial-state splittings are removed via $\overline{\text{MS}}$ QCD factorization by PDF redefinitions. In both evaluations the phase-space integration is performed with multichannel Monte Carlo generators [58] and adaptive weight optimization similar to the one implemented in LUSIFER [59].

In the following we consider the process $pp \to t\bar{t}b\bar{b} + X$ at the LHC, i.e., for $\sqrt{s} = 14$ TeV. For the top-quark mass, renormalized in the on-shell scheme, we take the numerical value $m_t = 172.6$ GeV [60]. All other QCD partons (including b quarks) are treated as massless particles, and collinear final-state configurations, which give rise to singularities, are recombined into IR-safe jets using a k_T algorithm [61]. Specifically, we adopt the k_T algorithm of Ref. [62] and recombine all final-state b quarks and gluons with pseudorapidity $|\eta| < 5$ into jets with separation $\sqrt{\Delta\phi^2 + \Delta y^2} > D = 0.8$ in the rapidity–azimuthal-angle plane. Requiring two b-quark jets, this also avoids collinear singularities resulting from the splitting of gluons into (massless) b quarks. Motivated by the search for a $t\bar{t}H(H \to b\bar{b})$ signal at the LHC [4,5], we impose the following additional cuts on the transverse momenta, the rapidity, and the invariant mass of the two (recombined) b jets: $p_{T,b} > 20$ GeV, $|y_b| < 2.5$, and $m_{b\bar{b}} > m_{b\bar{b},\text{cut}}$. We plot results either as a function of $m_{b\bar{b},\text{cut}}$ or for $m_{b\bar{b},\text{cut}} = 0$. Note, however, that the jet algorithm and the requirement of having two b jets with finite $p_{T,b}$ in the final-state sets an effective lower limit on the invariant mass $m_{b\bar{b}}$ of roughly 20 GeV. The outgoing (anti)top quarks are neither affected by the jet algorithm nor by phase-space cuts.

We consistently use the CTEQ6 [63,64] set of PDF's; i.e., we take CTEQ6L1 PDF's with a one-loop running α_s in LO and CTEQ6M PDFs with a two-loop running α_s in NLO, but the suppressed contributions from b quarks in the initial state have been neglected. The number of active flavours is $N_F = 5$, and the respective QCD parameters are $\Lambda_5^{\text{LO}} = 165$ MeV and $\Lambda_5^{\overline{\text{MS}}} = 226$ MeV. In the renormalization of the strong coupling constant the top-quark loop in the gluon self-energy is subtracted at zero momentum. In this scheme, the running of α_s is generated solely by the contributions of the light-quark and gluon loops. By default, we set the renormalization and factorization scales, μ_R and μ_F, to the common value $\mu_0 = m_t + m_{b\bar{b},\text{cut}}/2$.

In Fig. 2 we show the scale dependence of the LO and NLO cross sections upon varying the renormalization and factorization scales in a uniform or an antipodal way. We observe an appreciable reduction of the scale uncertainty upon going from LO to NLO. Varying the scale up or down by a factor 2 changes the cross section by 70% in LO and by 34% in NLO. At the central scale, the full pp cross section receives a very large NLO correction of 77%, which is mainly due to the gluonic initial states.

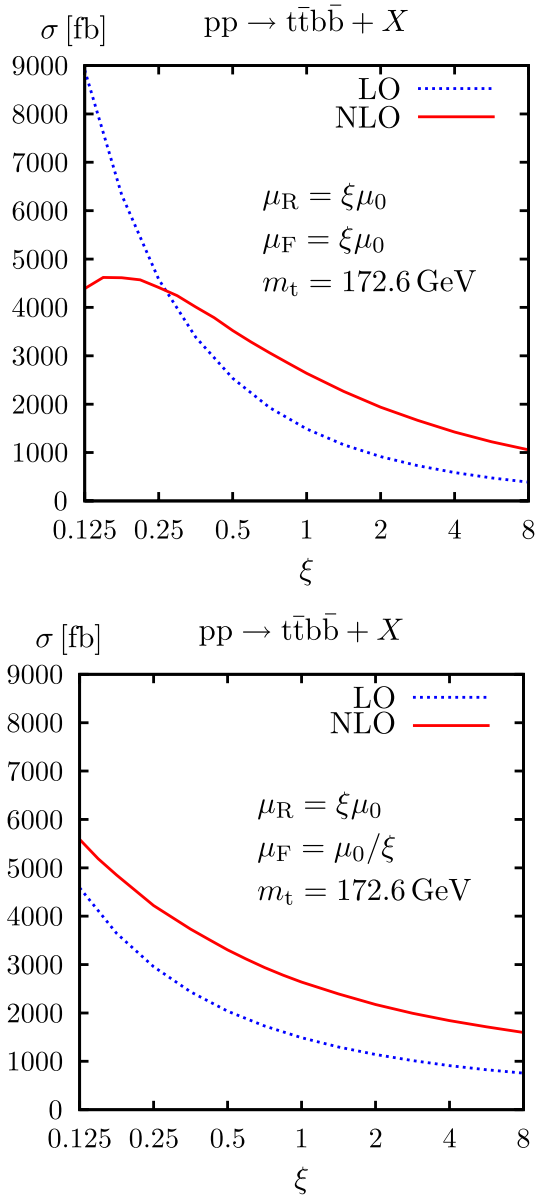

FIG. 2 (color online). Dependence of the LO and NLO cross sections of $pp \to t\bar{t}b\bar{b} + X$ at the LHC for $m_{b\bar{b},\mathrm{cut}} = 0$ and $\mu_0 = m_t$.

Introducing a veto on extra jets by requiring $p_{T,\mathrm{jet}} < 50$ GeV reduces the K factor to roughly 1.2. For the $q\bar{q}$ channel we found a very small correction of 2.5% [1]. The full LO and NLO cross sections are given by $\sigma_{\mathrm{LO}} = 1488.8(1.2)$ fb and $\sigma_{\mathrm{NLO}} = 2638(6)$ fb, where the numbers in parentheses are the errors of the Monte Carlo integration for 2×10^7 events.

Figure 3 shows the LO and NLO cross sections as a function of the cut $m_{b\bar{b},\mathrm{cut}}$ on the $b\bar{b}$ invariant mass, where the bands indicate the effect from a uniform or antipodal rescaling of μ_R and μ_F by factors $1/2$ and 2. The shown LO and NLO bands overlap in the whole considered range in $m_{b\bar{b},\mathrm{cut}}$, which is motivated by the search for a low-mass

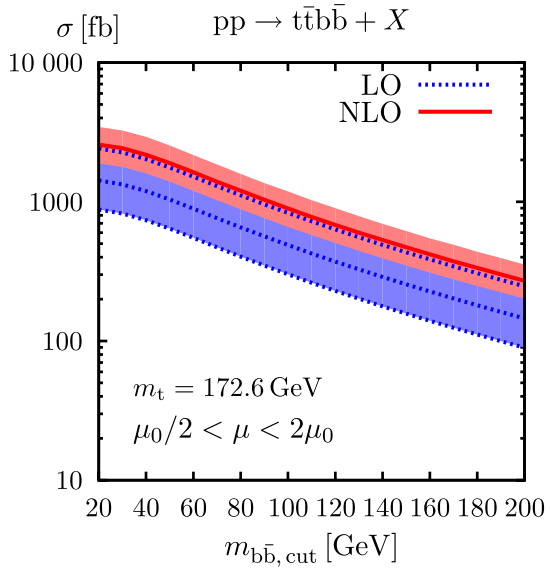

FIG. 3 (color online). LO and NLO cross sections for $pp \to t\bar{t}b\bar{b} + X$ at the LHC as function of $m_{b\bar{b},\mathrm{cut}}$, with the bands indicating the scale dependence by varying μ_R and μ_F by factors $1/2$ and 2 in a uniform or antipodal way ($\mu_0 = m_t + m_{b\bar{b},\mathrm{cut}}/2$).

Higgs boson. In contrast to the pure $q\bar{q}$ channel [1], the NLO corrections to the full pp process induce only a moderate distortion of the functional dependence on $m_{b\bar{b},\mathrm{cut}}$. The reduction of the scale uncertainty from about $\pm 70\%$ to $\pm 33\%$ and the large impact of the NLO correction hold true for the considered range in $m_{b\bar{b},\mathrm{cut}}$.

In summary we have presented first results on the full NLO prediction for the process $pp \to t\bar{t}b\bar{b} + X$ at the LHC. The NLO corrections appreciably reduce the unphysical scale dependence of the LO cross section, but at the same time enhance the cross section by a K factor of about 1.8 for the usual scale choice. This large correction factor can be strongly reduced by imposing a veto on hard jets. It will be interesting to see how these NLO results influence the signal significance of $t\bar{t}$-Higgs production with a Higgs boson decaying into a $b\bar{b}$ pair, to which direct $t\bar{t}b\bar{b}$ production represents a serious background.

On the technical side the presented calculation constitutes the first complete NLO prediction for a hadronic process of the type $2 \to 4$ particles. Speed and stability of the evaluation show good performance of the Feynman-diagrammatic approach that is augmented by dedicated reduction methods of tensor loop integrals for exceptional phase-space regions.

On a single 3 GHz Intel Xeon processor, the evaluation of the virtual corrections for $gg \to t\bar{t}b\bar{b}$ (including sums over color and polarization states) takes about 160 ms per phase-space point. This remarkably high speed suggests that the employed reduction method might turn out to be a very efficient tool for various other multiparticle processes at the LHC.

We thank Thomas Hahn for technical help in structuring the very long source code, as well as M. Mangano and C. Papadopoulos for helpful discussions on off-shell recursion relations. This work is supported in part by the European Community's Marie-Curie Research Training Network under contract MRTN-CT-2006-035505 ''Tools and Precision Calculations for Physics Discoveries at Colliders'' and the Japan Society for the Promotion of Science.

[1] A. Bredenstein *et al.*, J. High Energy Phys. 08 (2008) 108.
[2] ATLAS Collaboration, CERN, Technical Design Report No. CERN-LHCC-99-15, 1999, Vol. 2.
[3] V. Drollinger, T. Müller, and D. Denegri, arXiv:hep-ph/0111312.
[4] J. Cammin and M. Schumacher, Report No. ATL-PHYS-2003-024, 2003.
[5] S. Cucciarelli *et al.*, CMS Note Report No. 2006/119, 2006.
[6] D. Benedetti *et al.*, J. Phys. G **34**, N221 (2007).
[7] G. Aad *et al.* (ATLAS Collaboration), arXiv:0901.0512.
[8] W. Beenakker *et al.*, Phys. Rev. Lett. **87**, 201805 (2001).
[9] W. Beenakker *et al.*, Nucl. Phys. **B653**, 151 (2003).
[10] S. Dawson *et al.*, Phys. Rev. D **67**, 071503 (2003).
[11] S. Dawson *et al.*, Phys. Rev. D **68**, 034022 (2003).
[12] S. Dittmaier, P. Uwer, and S. Weinzierl, Phys. Rev. Lett. **98**, 262002 (2007).
[13] S. Dittmaier, P. Uwer, and S. Weinzierl, Eur. Phys. J. C **59**, 625 (2009).
[14] A. Lazopoulos *et al.*, Phys. Lett. B **666**, 62 (2008).
[15] C. Buttar *et al.*, arXiv:hep-ph/0604120.
[16] Z. Bern *et al.* (NLO Multileg Working Group), arXiv:0803.0494.
[17] A. Ferroglia *et al.*, Nucl. Phys. **B650**, 162 (2003).
[18] A. Denner and S. Dittmaier, Nucl. Phys. **B658**, 175 (2003).
[19] W. T. Giele and E. W. N. Glover, J. High Energy Phys. 04 (2004) 029.
[20] W. Giele, E. W. N. Glover, and G. Zanderighi, Nucl. Phys. B, Proc. Suppl. **135**, 275 (2004).
[21] T. Binoth *et al.*, J. High Energy Phys. 10 (2005) 015.
[22] A. Denner and S. Dittmaier, Nucl. Phys. **B734**, 62 (2006).
[23] T. Binoth *et al.*, arXiv:0810.0992.
[24] Z. Bern, L. J. Dixon, and D. A. Kosower, Ann. Phys. (Leipzig) **322**, 1587 (2007).
[25] G. Ossola, C. G. Papadopoulos, and R. Pittau, Nucl. Phys. **B763**, 147 (2007).
[26] R. K. Ellis, W. T. Giele, and Z. Kunszt, J. High Energy Phys. 03 (2008) 003.
[27] G. Ossola, C. G. Papadopoulos, and R. Pittau, J. High Energy Phys. 03 (2008) 042.
[28] W. T. Giele, Z. Kunszt, and K. Melnikov, J. High Energy Phys. 04 (2008) 049.
[29] C. F. Berger *et al.*, Phys. Rev. D **78**, 036003 (2008).
[30] W. T. Giele and G. Zanderighi, J. High Energy Phys. 06 (2008) 038.
[31] A. Lazopoulos, arXiv:0812.2998.
[32] J.-C. Winter and W. T. Giele, arXiv:0902.0094.
[33] R. K. Ellis *et al.*, J. High Energy Phys. 01 (2009) 012.
[34] A. van Hameren, C. G. Papadopoulos, and R. Pittau, arXiv:0903.4665.
[35] R. K. Ellis, K. Melnikov, and G. Zanderighi, J. High Energy Phys. 04 (2009) 077.
[36] C. F. Berger *et al.*, Phys. Rev. Lett. **102**, 222001 (2009).
[37] A. Denner *et al.*, Phys. Lett. B **612**, 223 (2005).
[38] A. Denner *et al.*, Nucl. Phys. **B724**, 247 (2005).
[39] G. Lei *et al.*, Phys. Lett. B **654**, 13 (2007).
[40] T. Reiter, arXiv:0903.4648.
[41] J. Küblbeck, M. Böhm, and A. Denner, Comput. Phys. Commun. **60**, 165 (1990).
[42] T. Hahn, Comput. Phys. Commun. **140**, 418 (2001).
[43] T. Hahn and M. Perez-Victoria, Comput. Phys. Commun. **118**, 153 (1999).
[44] G. Passarino and M. J. G. Veltman, Nucl. Phys. **B160**, 151 (1979).
[45] G. 't Hooft and M. J. G. Veltman, Nucl. Phys. **B153**, 365 (1979).
[46] W. Beenakker and A. Denner, Nucl. Phys. **B338**, 349 (1990).
[47] S. Dittmaier, Nucl. Phys. **B675**, 447 (2003).
[48] J. Alwall *et al.*, J. High Energy Phys. 09 (2007) 028.
[49] S. Dittmaier, Phys. Rev. D **59**, 016007 (1998).
[50] F. A. Berends and W. T. Giele, Nucl. Phys. **B306**, 759 (1988).
[51] F. Caravaglios and M. Moretti, Phys. Lett. B **358**, 332 (1995).
[52] P. Draggiotis, R. H. P. Kleiss, and C. G. Papadopoulos, Phys. Lett. B **439**, 157 (1998).
[53] S. Catani *et al.*, Nucl. Phys. **B627**, 189 (2002).
[54] S. Catani and M. H. Seymour, Nucl. Phys. **B485**, 291 (1997).
[55] S. Dittmaier, Nucl. Phys. **B565**, 69 (2000).
[56] L. Phaf and S. Weinzierl, J. High Energy Phys. 04 (2001) 006.
[57] R. Frederix, T. Gehrmann, and N. Greiner, J. High Energy Phys. 09 (2008) 122.
[58] J. Hilgart, R. Kleiss, and F. Le Diberder, Comput. Phys. Commun. **75**, 191 (1993).
[59] S. Dittmaier and M. Roth, Nucl. Phys. **B642**, 307 (2002).
[60] Tevatron Electroweak Working Group, arXiv:0803.1683.
[61] S. Catani, Y. L. Dokshitzer, and B. R. Webber, Phys. Lett. B **285**, 291 (1992).
[62] G. C. Blazey *et al.*, arXiv:hep-ex/0005012.
[63] J. Pumplin *et al.*, J. High Energy Phys. 07 (2002) 012.
[64] D. Stump *et al.*, J. High Energy Phys. 10 (2003) 046.